Thermally activated antibiotic production by probiotic bacteria for pathogen elimination

Sourik Dey[1], Carsten E. Seyfert[2,3], Claudia Fink-Straube[1], Andreas M. Kany[2,3], Rolf Müller[2,3], Shrikrishnan Sankaran*[1]

[1] INM - Leibniz Institute for New Materials, Campus D2 2, 66123 Saarbrücken, Germany

[2] Microbial Natural Products, Helmholtz Institute for Pharmaceutical Research Saarland (HIPS), Helmholtz Centre for Infection Research (HZI) and Department of Pharmacy at Saarland University, Campus Building E8.1, 66123 Saarbrücken (Germany)

[3] German Centre for Infection Research (DZIF), partner site Hannover-Braunschweig, Germany

*E-mail: **shrikrishnan.sankaran@leibniz-inm.de**

Abstract

Engineered bacterial therapeutics is a rapidly emerging field in which bacteria are genetically engineered to produce and deliver therapeutic compounds at the body site of use. They offer the advantages of being able to produce biopharmaceutical drugs on the spot and control drug release time and dosage through genetic switches to treat a variety of diseases, including infections, inflammatory diseases, and cancer. However, a major challenge in the field is achieving drug production rates for effectively treating diseases. This is especially true when combining genetic switches with heterologous gene expression. This study presents an expression strategy to overcome this challenge as part of developing thermo-switchable production of a novel antibiotic, darobactin, in probiotic *Escherichia coli* Nissle 1917. While thermo-switchable promoters produced ineffective levels of darobactin, the T7 promoter enabled production of pathogen-inhibitory levels although it was highly leaky. Thus, parts from both switches were combined to create a thermo-amplifier circuit that shows no detectable leakiness below 37 ^{o}C and releases sufficient darobactin at 40°C to inhibit the growth of a critically prioritized *Pseudomonas aeruginosa* pathogen.

Keywords – Probiotics, *E. coli* Nissle 1917, Darobactin, T7 RNA polymerase, Thermo-amplifier, Anti-bacterial

Introduction

The field of engineered bacterial therapeutics has gained significant momentum as a novel approach to treat challenging diseases (Maxmen 2017; Charbonneau et al, 2020; Liu et al., 2022). This emerging technology involves the genetic programming of bacteria to synthesize and administer therapeutic substances within the body. The potential applications span a wide spectrum of medical conditions including infections, inflammatory disorders and cancer (Kelly et al., 2020). A distinctive advantage of engineered bacterial therapeutics is their ability to generate complex bioactive molecules directly in the body. Furthermore, encoding of genetic switches in these therapeutic bacteria offers to regulate the timing and dosage of drug release. Through these unique possibilities, engineered bacterial therapeutics can achieve on-demand production of intricate and costly biopharmaceutical drugs directly at the required body-site, thus mitigating issues associated with storage, transportation, and drug stability. By encapsulating such bacteria in biocompatible materials, it is also possible to create smart self-replenishing drug-delivery devices to treat chronic diseases (Omer et al., 2022; Rodrigo-Navarro et al., 2021). Thus, engineered bacterial therapeutics offer the possibility to provide a tailored and patient-centric treatment approach.

However, as the field progresses, it grapples with significant hurdles, one of which is achieving the necessary production rates of therapeutic agents to effectively combat diseases (Zhou and Han, 2022). This challenge becomes even more pronounced when genetic switches are coupled with genes encoding the production of therapeutic compounds from different species. Striking a balance between robust drug synthesis and stringent control over production on demand requires considerable optimization of the genetic circuits and development of novel genetic modules (Kan et al., 2020). In recent studies, promoter engineering enabled thermally regulated expression and release of oncolytic nanobodies (Abedi et al., 2022) and tumor necrosis factor (TNF-α) (Li et al., 2022) from the probiotic *E. coli* Nissle 1917 (EcN) strain for treating solid tumors in mice models. While these studies achieved activation of bacterial gene expression within the host, the output was limited to the production and secretion of a single protein. In contrast only a few studies have addressed stimuli-responsive regulation of compounds produced

through enzyme cascades (Sankaran et al., 2019; Sugianto et al., 2023). These studies often reveal that the regulated production of such compounds is more challenging compared to single proteins due to greater leaky expression or lower output yields, especially when the product can be toxic to the host cell at high concentrations.

One such high-value enzymatically synthesized compound that has recently risen to prominence is darobactin, a novel antibiotic (Imai et al., 2019). This antibiotic has shown potential in eliminating harmful Gram-negative pathogens, including those that are highly virulent and antibiotic resistant (ESKAPE classification) (Imai et al., 2019; Seyfert et al., 2023a). The synthesis of darobactin is possible in *E. coli* and considerable efforts are underway to improve production yields for its economically viable upscaled manufacturing (Wuisan et al., 2021; Groß et al., 2021; Li et al., 2023; Seyfert et al., 2023b). As a ribosomally synthesized and post-translationally modified peptide (RiPP), the darobactin operon includes the DarA peptide followed by DarBCDE enzymes that modify it into its active form and transport it out of the cell. Complementary to the efforts of improving darobactin production yields, developing an engineered bacterial therapeutic that produces and releases the drug directly in the body would offer a promising alternative strategy for the applicability of this drug with the previously mentioned benefits.

In this study, we engineered the probiotic *E. coli* strain for thermo-switchable darobactin production (37 ^{o}C OFF, 40 ^{o}C ON). This approach avoids continuous release of the antibiotic from the engineered bacteria, which could lead to the development of resistance (Imai et al., 2019). Notably, we faced the previously mentioned challenges of leaky and insufficient expression in different genetic circuits to achieve such switching. We were able to simultaneously resolve both issues by developing a genetic amplification strategy that resulted in a thermo-amplifier circuit with undetectable leakiness and darobactin production levels sufficient for inhibiting the growth of pathogenic *Pseudomonas aeruginosa* PAO1.

Results

Functional characterization of inducible darobactin production

At first, an endotoxin-free *E. coli* strain, ClearColi (Mamat et al., 2015), was engineered to produce and secrete darobactin by transforming it with the pNOSO-darABCDE plasmid (Groß et al., 2021). In this plasmid, the DarA propeptide is encoded downstream of an IPTG-inducible lacO-operated T7 promoter and the DarBCDE enzyme cascade is constitutively expressed (Figure 1A). As highlighted by Groß and coworkers before, *darBCD* encode for a permease protein (DarB), membrane fusion protein (DarC) and ATP-binding protein (DarD), all together comprising a tripartite efflux pump facilitating darobactin export from the bacterial chassis. The DarE protein is a radical *S*-adenosyl-L-methionine (SAM) enzyme which catalyses the formation of the ether and C–C crosslinking in the heptapeptide core structure (W^1–N^2–W^3–S^4–K^5–S^6–F^7) of the DarA propeptide (Nguyen et al., 2022). The darobactin amount secreted by this strain in Formulated Medium (FM) at 37°C following 24 h of IPTG induction (0.5 mM) was ~2.5 µg/mL, detected directly in the medium by Electrospray ionization–mass spectrometry (ESI-MS). This corresponded to the previously reported minimum inhibitory concentrations (MIC) determined for the commonly tested model pathogenic strain, *P. aeruginosa* PAO1 (>2 µg/mL) (Imai et al., 2019). However, even without IPTG induction, the system was considerably leaky and produced ~1 µg/mL of darobactin in FM (Figure 1B). To achieve thermoresponsive production and secretion of darobactin, its biosynthetic gene cluster (BGC) was cloned into the thermogenetic pTlpA39-mWasabi plasmid (#Addgene 86116). In this system, a thermosensitive repressor (TSR) undergoes dimerization and represses the P_{tlpA} promoter at temperatures below 39°C. Above this threshold temperature, the repressor reverts to its monomeric state allowing P_{tlpA} promoter-based gene expression (Piraner et al., 2017). For the thermally activated constructs, *darA* was encoded downstream of the P_{tlpA} promoter. The DarBCDE enzyme cascade was constitutively expressed by the promoter P_{TN5} as in the pNOSO-darABCDE plasmid. Notably, the pNOSO vector backbone has a medium-copy number p15A replicon, whereas the pTlpA39 plasmid is based on a high-copy number pMB1 replicon (pUC). Thus, two plasmids encoding thermoresponsive darobactin production modules were constructed with each of these replicons and annotated as p15A-Tlp-DarA and pUC-

Tlp-DarA respectively (Figure 1C). While no darobactin was detected in the medium of ClearColi containing p15A-Tlp-DarA after 24 h incubation (at both 37°C and 40°C), the strain containing pUC-Tlp-DarA released detectable levels of darobactin in the culture medium at both incubation temperatures. The resulting darobactin concentration in the medium for the pUC-Tlp-DarA construct at 40°C (~0.13 µg/mL) was ~4 fold higher than that observed at 37°C (~0.03 µg/mL) (Figure 1D). Although the darobactin concentrations were significantly lower than the desired MIC for inhibiting Gram-negative pathogenic strains, thermoresponsive production was confirmed. This encouraged us to optimize the performance of the gene circuit based on the high-copy number plasmid, pUC-Tlp-DarA.

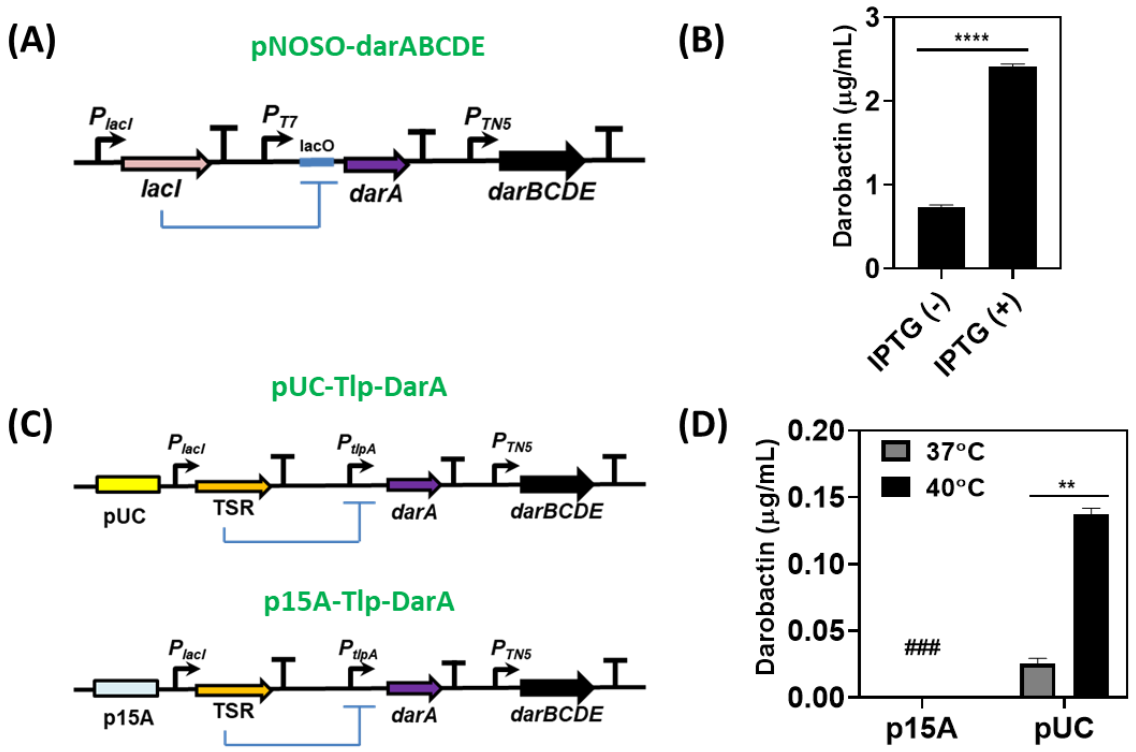

Figure 1. (A) Schematic representation of the pNOSO-darABCDE gene circuit. (B) Darobactin concentration in the liquid medium (in µg/mL) for the pNOSO-darABCDE construct in Clearcoli BL21 (DE3) strain after 24 h of incubation. The bacteria were induced with 500 µM of IPTG at OD_{600} =0.4 in Formulated Media (FM) supplemented with 50 µg/mL kanamycin. The error bars represent standard deviation based on three independent measurements ($p < 0.0001$ as calculated by paired t-test) (C) Schematic representation of the thermoresponsive darobactin production gene circuits based on high—copy (pUC-Tlp-DarA) and mid-copy (p15A-Tlp-DarA) number replication origin. The thermosensitive repressor (TSR) represses P_{tlpA} promoter at physiological temperature (37°C) and is derepressed at temperatures beyond >39°C. (D) Darobactin

concentration in the liquid medium (in µg/mL) for the p15A and pUC origin based Tlp-DarA gene circuits after 24 h of incubation at 37°C and 40°C. (###) represents darobactin concentration lower than the Limit of Detection (LOD) by ESI-MS. The pUC-Tlp-DarA circuit produced higher darobactin levels (~4 fold change) at 40°C in comparison to 37°C. The error bars represent standard deviation based on three independent measurements (p =0.0016 as calculated by paired t-test)

To determine the expression strengths and fold-changes of the inducible promoters, the *darA* was replaced by a red fluorescent reporter gene (*mCherry*) in the pNOSO and pUC-Tlp vector backbone without altering any other coding sequence (CDS) to create pNOSO-mCherry (Figure S1A) and pUC-Tlp-mCherry (Figure S1B), respectively. Post IPTG induction, it was observed that mCherry production in pNOSO-mCherry (P_{T7} promoter) was only ~2.5 fold higher than the uninduced control (Figure S1E), whereas the pUC-Tlp-mCherry (P_{tlpA} promoter) circuit had a ~40-fold increase in fluorescence at 40°C compared to 37°C (Figure S1F). However, the pUC-Tlp-DarA circuit produced an overall higher relative fluorescence unit (RFU) at 40°C (Figure S1D) than the IPTG induced pNOSO-mCherry circuit (Figure S1C). This contrasting result suggests that the genetic circuits encoding darobactin production might be influenced by alternate factors like the *darA:darE* transcript ratio (Wuisan et al., 2021) or intracellular toxicity (Groß et al., 2021; Seyfert et al., 2023b), rather than the production rate of DarA alone. In accordance with our observations regarding pNOSO-darABCDE, there was considerable basal level expression of mCherry protein observed in pNOSO-mCherry samples grown without any IPTG supplementation. On the other hand, mCherry expression was tightly regulated by the TSR protein in pUC-Tlp-mCherry below the threshold temperature in line with our previous report (Basaran et al., 2023). This shows that TSR protein-based gene regulation is more effective than the conventional lacI repressor protein which is known for its inability to mediate strong repression (Singha et al., 2017).

One major factor that distinguishes darobactin production from that of mCherry is that darobactin could exert a detrimental effect on the growth of the bacterial host (Imai et al., 2019, Groß et al. 2021). To validate this hypothesis, the constitutive expression of darobactin was tested in Clearcoli by exchanging the thermoresponsive elements in pUC-Tlp-DarA with the P_{T7} promoter upstream of the d*arA* gene (pT7-DarA) that can be

strongly driven by the cognate T7 RNA Polymerase (T7RNAP) genomically encoded in Clearcoli. As expected, this caused a significant reduction in the bacterial biomass (~100 mg per 25 mL of liquid culture) in comparison to the IPTG induced pNOSO-darABCDE construct (~430 mg per 25 mL of liquid culture) when cultivated at 37°C for 24 h (Figure S2A). This is possibly caused by constitutive expression of darobactin by the pT7-DarA construct leading to a significant metabolic burden on the producer strain. This also resulted in a considerable reduction of the overall darobactin concentration (~0.09 µg/mL) observed in the liquid medium compared to the pNOSO-DarABCDE construct (Figure S2B). Thus, inducible expression of darobactin is essential to achieve higher darobactin concentration without compromising the system's overall performance.

Selection of an efficient antibiotic supplementation-free plasmid retention strategy

Before further optimization of thermoresponsive darobactin production, strategies to retain the pUC-Tlp-DarA plasmid in an antibiotic supplementation-free manner were tested. Earlier reports on engineered probiotics have highlighted the importance of maintaining the genetic stability of the heterologous protein encoding genes during bacterial growth (Landry and Tabor, 2018). Although, the most preferred route to achieve genetic stability is to integrate the heterologous genes in the chassis genome, studies have shown that this could significantly reduce the overall production (Aggarwal et al., 2020) and secretion (Durmusoglu et al., 2023) levels of recombinant proteins. As in our case, we were unable to observe darobactin production in the liquid cultures, using a medium-copy vector backbone (p15A ori), we decided not to proceed with genomic integration approaches for our genetic circuits. As low but detectable levels of darobactin were observed in the liquid cultures for the genetic circuit based on the high-copy number vector backbone (pUC ori), we decided to employ plasmid retention strategies that would not require additional antibiotic supplementation in the growth medium. To realize antibiotic-free retention of a plasmid encoding darobactin-production, we tested two commonly employed plasmid retention strategies based on nutrient auxotrophy (Hwang et al., 2017) and toxin-antitoxin dependent post segregational killing (Gurbatri et al., 2020). For auxotrophy based plasmid retention, the alanine racemase genes (*alr* and *dad*X) essential for alanine biosynthesis in ClearColi were deleted from the bacterial

genome to select for the double knockout Δ*alr* Δ*dadX* Clearcoli strain that could be only grown when externally supplemented with D-alanine. The *alr* gene with its native promoter was amplified from *E. coli* DH5α genomic DNA and cloned into the vector backbone of pUC-Tlp-DarA to create the pTlp-DarA-alr construct (Figure 2A) that would support plasmid retention when the bacteria are grown in the absence of D-alanine. For the toxin-antitoxin (TA) based plasmid retention strategy, a type II TA gene pair, *txe-axe*, originally isolated from *Enterococcus faecium* (Grady and Hayes, 2003), was used. Recent studies have shown that the *txe-axe* TA system was able to stably retain engineered plasmids in *E. coli* over several generations in *in-vitro* experiments (Fedorec et al., 2019), making it a suitable option as well for *in-vivo* assessment (Harimoto et al., 2022). The *txe-axe* gene pair was amplified from the pUC-GFP-AT (Addgene #133306) plasmid and cloned into pUC-Tlp-DarA to create the pTlp-DarA-AT plasmid (Figure 2C). The antibiotic-free retention plasmids, pTlp-DarA-alr and pTlp-DarA-AT, were transformed in Clearcoli Δ*alr*Δ*dadX* and unmodified Clearcoli strains, respectively and cultivated in FM for 24 h, both with and without antibiotic supplementation (100 µg/mL ampicillin). Post incubation, no significant difference of darobactin concentrations (liquid medium) was observed for the strains containing either pTlp-DarA-alr (Figure 2B) or pTlp-DarA-AT (Figure 2D) in the absence of the antibiotic when compared to in the presence of it. The fold change in darobactin production in response to the incubation temperatures also remained unaffected during this period. These results suggested that both the retention strategies could effectively retain the engineered plasmids during cellular growth and simultaneous darobactin production for 24 h. As no distinct advantage of either strategy was noticed in terms of darobactin production in the tested temporal period, preference was given to the *txe-axe* TA system for its ability to be used across several related *E. coli* strains without them having to undergo any permanent genomic modifications.

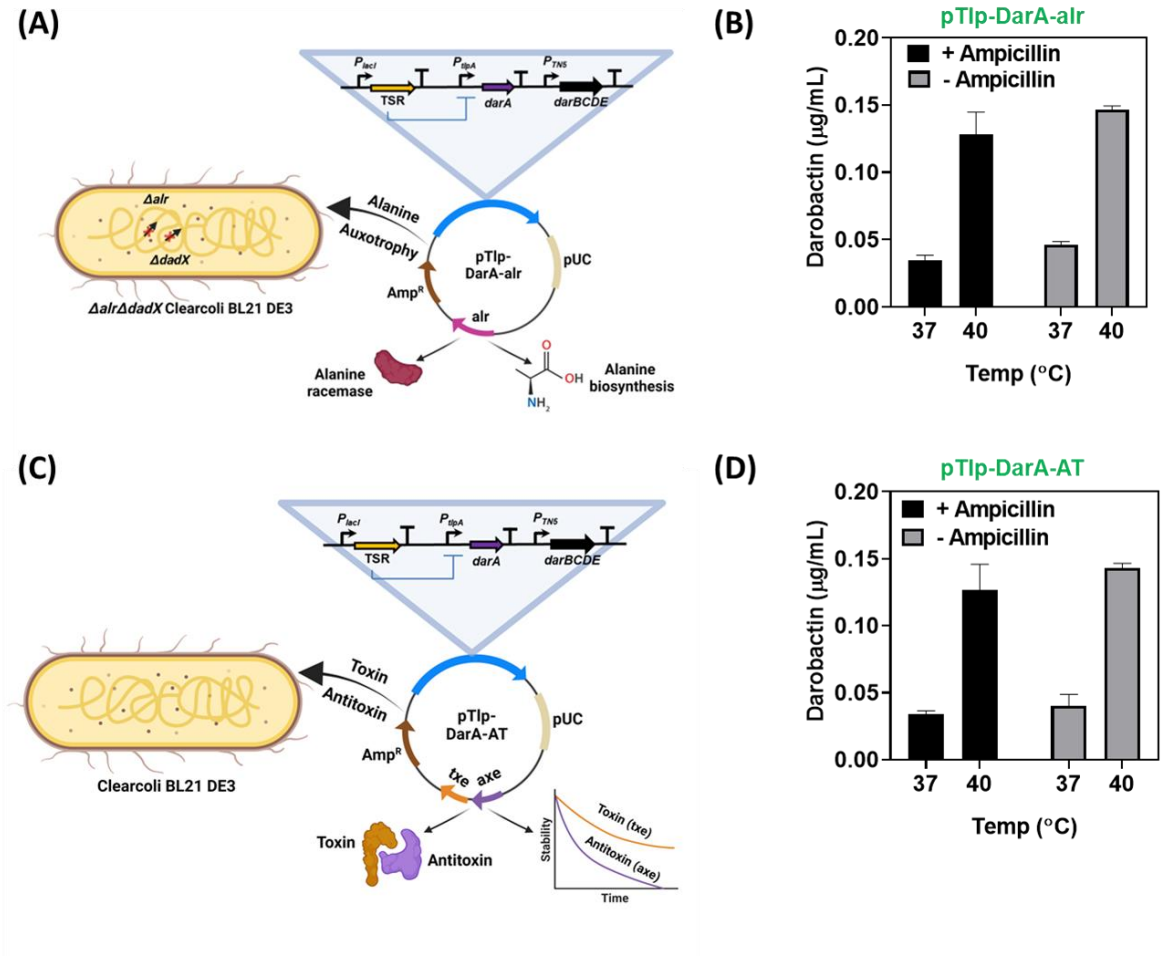

Figure 2. (A) Schematic representation of the pTlp-DarA-alr construct transformed in Δ*alr* Δ*dad*X Clearcoli BL21 DE3. The integration of the alanine racemase (*alr*) gene in the pUC-Tlp-DarA vector backbone mediates alanine biosynthesis in the auxotrophic strain. (B) Darobactin concentration in the liquid medium (in µg/mL) for the pTlp-DarA-alr construct after 24 h of incubation at 37°C and 40°C, both with and without ampicillin (100 µg/mL) supplementation. The error bars represent standard deviation based on three independent measurements. (C) Schematic representation of the pTlp-DarA-AT construct transformed in Clearcoli BL21 (DE3). The integration of the txe toxin - axe antitoxin (TA) gene pair in the pUC-Tlp-DarA vector backbone mediates plasmid retention by its controlled endoribonuclease activity and differential protein stability rates. (D) Darobactin concentration in the liquid medium (in µg/mL) for the pTlp-DarA-AT construct after 24 h of incubation at 37°C and 40°C, both with and without ampicillin (100 µg/mL) supplementation. The error bars represent standard deviation based on three independent measurements.

Optimized Genetic Circuit to Increase Darobactin Production

From the previous results, it was determined that the P_{T7} promoter with the cognate T7RNAP was able to support high levels of darobactin production but poor inducible fold-changes. On the other hand, the P_{tlpA} promoter along with its TSR was found to mediate thermoresponsive darobactin production with an appreciable fold change between 37 ^{o}C and 40 ^{o}C but poor overall concentration in the liquid medium. To increase the darobactin concentration while maintaining thermoresponsive production, we combined components of both inducible systems to design a thermo-amplifier circuit (pTAMP). In this genetic circuit, *darA* gene expression is mediated by the P_{T7} promoter and the production of its cognate T7RNAP [amplified from the mBP-T7RNAP plasmid (Addgene #74096)] is controlled by the TSR regulated P_{tlpA} promoter (Figure 3A). Notably, this circuit could not be tested in ClearColi, since the constitutively expressed *t7-RNAP* gene is integrated in the genome of this strain. Thus, as an alternative, we chose the probiotic EcN strain, which is the prime *E. coli* strain being engineered for living therapeutic applications (Effendi et al., 2022; Yu et al., 2023). We determined that EcN is able to produce darobactin when transformed with pTlp-DarA-AT. The darobactin concentration after 24 h incubation in FM (liquid medium) without antibiotic supplementation was found to be ~ 0.02 µg/mL and ~0.07 µg/mL at 37°C and 40°C, respectively (Figure S3). This showed that the darobactin concentrations from EcN is very similar to that of the ClearColi strain and the fold change at the higher temperature is only ~3x. rt-PCR analysis further revealed no significant *darA* mRNA upregulation by the P_{tlpA} promoter of pTlp-DarA-AT at 40 ^{o}C (11.6 ± 0.3 cycles) compared to 37 ^{o}C (11.5 ±1.7 cycles) (Figure S4). This could explain the overall low darobactin concentration detected in FM by the P_{tlpA} promoter driven constructs. Surprisingly, when the thermo-amplifier circuit was constructed in a plasmid (pTAMP-DarA-AT) and tested in EcN, drastic improvement in the darobactin concentration (liquid medium) was observed at 40°C (~4.05 µg/mL), while its presence was below the detection limit of 0.01 µg/mL at 37°C after 24 h incubation in FM (Figure 3B). This thermo-regulation was further supported by rtPCR analysis that revealed gene expression levels of *darA* and *t7-RNAP* to be ~19 and ~9 fold higher at 40°C than at 37°C, respectively (Figure 3C, Figure 3D). Furthermore, the quantification cycle (Cq) value of *darA* at 40 ^{o}C for the pTAMP-DarA-AT construct was 8.1 ± 1.2 cycles, which formed the

logical basis for obtaining a higher darobactin concentration (liquid medium) in comparison to the pTlp-DarA-AT construct.

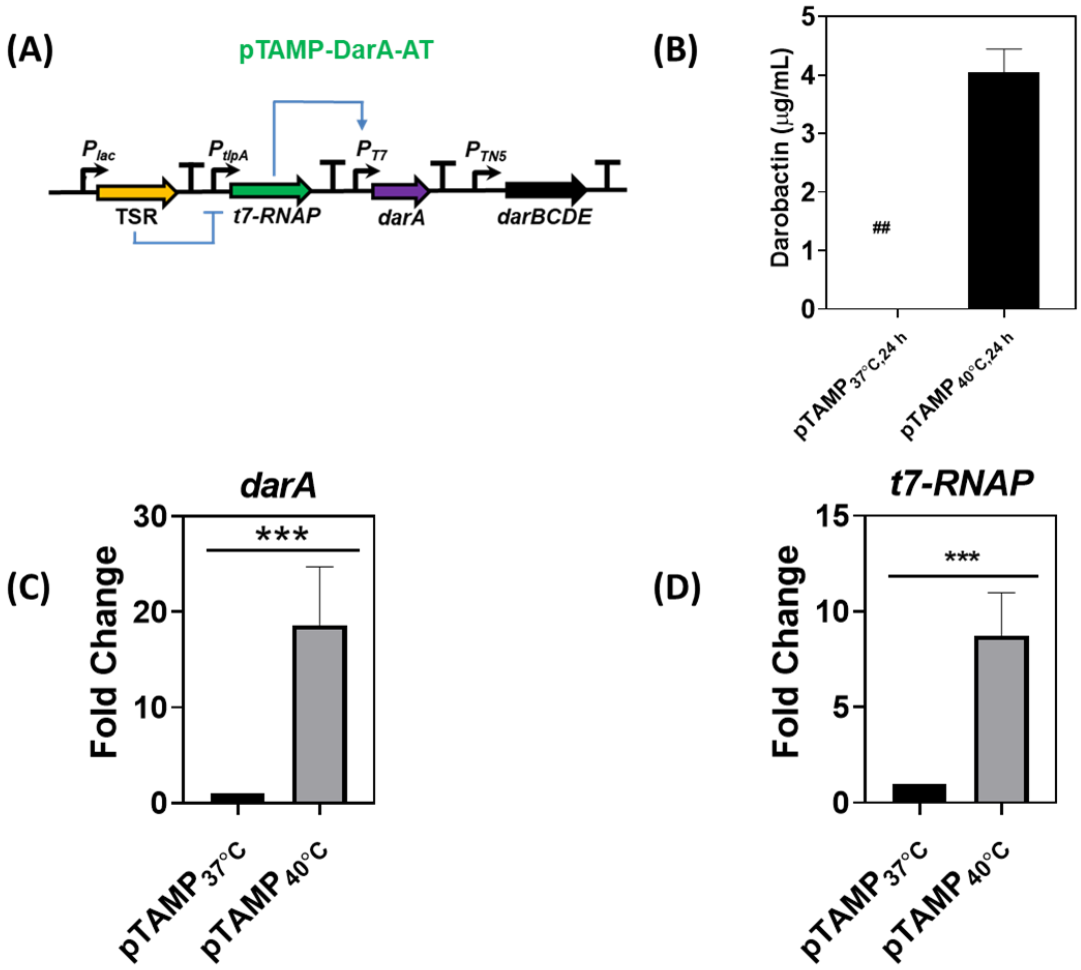

Figure 3. (A) Schematic representation of the pTAMP-DarA-AT genetic circuit. The TSR represses the *t7-RNAP* gene at incubation temperatures <39°C, beyond which the TSR de-repression leads to *t7-RNAP* expression and P_{T7} promoter based darobactin production. (B) Darobactin concentration in the liquid medium (in µg/mL) for the pTAMP-DarA-AT construct in *E. coli* Nissle 1917 (EcN) after 24 h of incubation at 37°C and 40° C respectively. The error bars represent standard deviation based on three independent measurements. (##) represents darobactin concentrations lower than the Limit of Detection (LOD) by ESI-MS. (C) Fold change in *darA* gene expression driven by the P_{T7} promoter of pTAMP-DarA-AT construct in EcN at 37°C and 40°C after 6 h incubation. The error bars represent standard deviation based on six independent measurements (p =0.0009 as calculated by paired t-test) (D) Fold change in *t7-RNAP* gene expression driven by the P_{tlpA} promoter of pTAMP-DarA-AT construct in EcN at 37°C and 40°C after 6 h incubation. The error bars represent standard deviation based on six independent measurements (p =0.0004 as calculated by paired t-test)

It is to be noted that the darobactin levels in medium achieved with the EcN pTAMP-DarA-AT strain was nearly 1.6-fold higher than that obtained by IPTG inducible production in ClearColi achieved with pNOSO-darABCDE. This suggests that P_{T7} driven production of darobactin in EcN should be higher than it is in ClearColi. To verify this, pNOSO-darABCDE was transformed in the EcN-T7 strain (DSMZ 115365), in which the *t7-RNAP* gene is genomically integrated and constitutively expressed in EcN (Fiege and Frankenberg-Dinkel, 2020). The darobactin levels obtained from this EcN strain after 24 h IPTG induction in FM was over 3-fold higher (~8.15 µg/mL) than that from the ClearColi strain and over 2-fold higher than that from EcN pTAMP-DarA-AT. Furthermore, similar to what was observed with the ClearColi pNOSO-darABCDE strain, the corresponding EcN strain exhibited high basal level darobactin concentrations in the liquid medium (~4.7 µg/mL) even in the absence of the IPTG inducer (Figure S5). Thus, EcN is able to offer higher levels of darobactin production and the thermo-amplifier circuit is able to significantly reduce leaky production, while still supporting potentially sufficient levels of darobactin production for pathogen inhibition.

Since darobactin inhibits the growth of Gram-negative bacteria including *E. coli*, the effect of its overproduction in the EcN strain was studied in terms of growth rates. Although the growth rate of the pTAMP-DarA-AT containing EcN strain was slightly reduced compared to the pTlp-DarA-AT containing EcN strain and the wild type EcN, at both 37°C (Figure S6A) and 40°C (Figure S6B) incubation temperatures, there was no significant temporal delay observed for the strains to reach their maximal cell density. The growth curves also showed that all the strains had an exponential increase in their cell density up to 6 h, corresponding to their log phase beyond which slower growth rates were observed. This motivated us to determine whether inducing the bacterial cultures at 40°C for a shorter period of 6 h could lead them to produce detectable levels of darobactin concentration in the liquid medium. Following this, we cultivated the EcN pTAMP-DarA-AT strain in FM for 6 h at both the incubation temperatures of 37°C and 40°C. When we analyzed the filter sterilized supernatant for determining the darobactin concentration, we detected ~4.3 µg/mL darobactin (liquid medium) for the samples incubated at 40°C and could not detect darobactin for the 37°C samples (Figure 4A) as observed before with the cultures incubated for 24 h.

Encouraged by these results, we studied the ability of the secreted darobactin to inhibit growth of *P. aeruginosa* PAO1. Initially, MIC experiments conducted with pure darobactin showed that concentrations above ~2 µg/mL could prevent the growth of *P. aeruginosa* PAO1 in both liquid cultures (Figure S7A) and on agar based medium (Figure S7B), in accordance with previous studies (Groß et al., 2021). To test whether the darobactin secreted into the liquid medium from EcN pTAMP-DarA-AT could also exert a similar effect, filter-sterilized FM was collected from the cultures after 6 h and 24 h incubation, at 37 ºC and 40°C, respectively. The media from cultures incubated at 40 ºC were able to drastically inhibit *P. aeruginosa* PAO1 growth, whereas the samples collected from its 37°C counterparts failed to inhibit *P. aeruginosa* PAO1 growth (Figure 4B).

Another important factor that contributes to determining the therapeutic success of an engineered strain, is the retention capability of its recombinant plasmids over several cell generations (Mortzfeld et al., 2022). To determine whether the *txe-axe* TA module could mediate successful plasmid retention over several generations, the pTAMP-DarA-AT EcN strain was cultivated for ~50 consecutive generations, with and without ampicillin (100 µg/mL) supplementation. qPCR analysis of bacterial populations after 10 and 50 generations showed no significant differences in the mean ΔCq fold change for samples cultivated at 40°C with or without antibiotic supplementation (Figure 4C). This suggested that the TA system ensured that the bacteria retained the plasmid at similar copy numbers even after 50 generations of cell growth in the absence of antibiotic (ampicillin) supplementation.

Finally, we tested the darobactin production capacity of the EcN pTAMP-DarA-AT strain in the presence of bile stress, which is known to promote antibiotic resistance (Reen et al., 2016) and biofilm formation in *P. aeruginosa* PAO1 (Flynn et al., 2019). For this, EcN pTAMP-DarA-AT was incubated at 37°C and 40°C in FM supplemented with 0.3% (w/v) Bovine Bile for 24 h. Post incubation, the filter sterilized FM samples were co-incubated with *P. aeruginosa* PAO1 and measured for their growth inhibitory potential. Significant inhibition was observed for media collected from the 40°C cultures compared to the 37°C cultures (Figure 4D). This showed that stress induction by 0.3% (w/v) Bovine Bile did not

reduce the antibacterial activity of the filtered supernatant. Independent analysis showed that both the wild type EcN and pTAMP-DarA-AT (EcN) strain could tolerate and grow at high bovine bile concentrations up to 1.5 % (w/v), also mentioned in independent studies (Nakkarach et al., 2020). All together our engineered probiotic strain can therefore be a suitable option to be explored as a Live Biotherapeutic Product (LBP) to eventually prevent *P. aeruginosa* colonization in the gut (Wheatley et al., 2022).

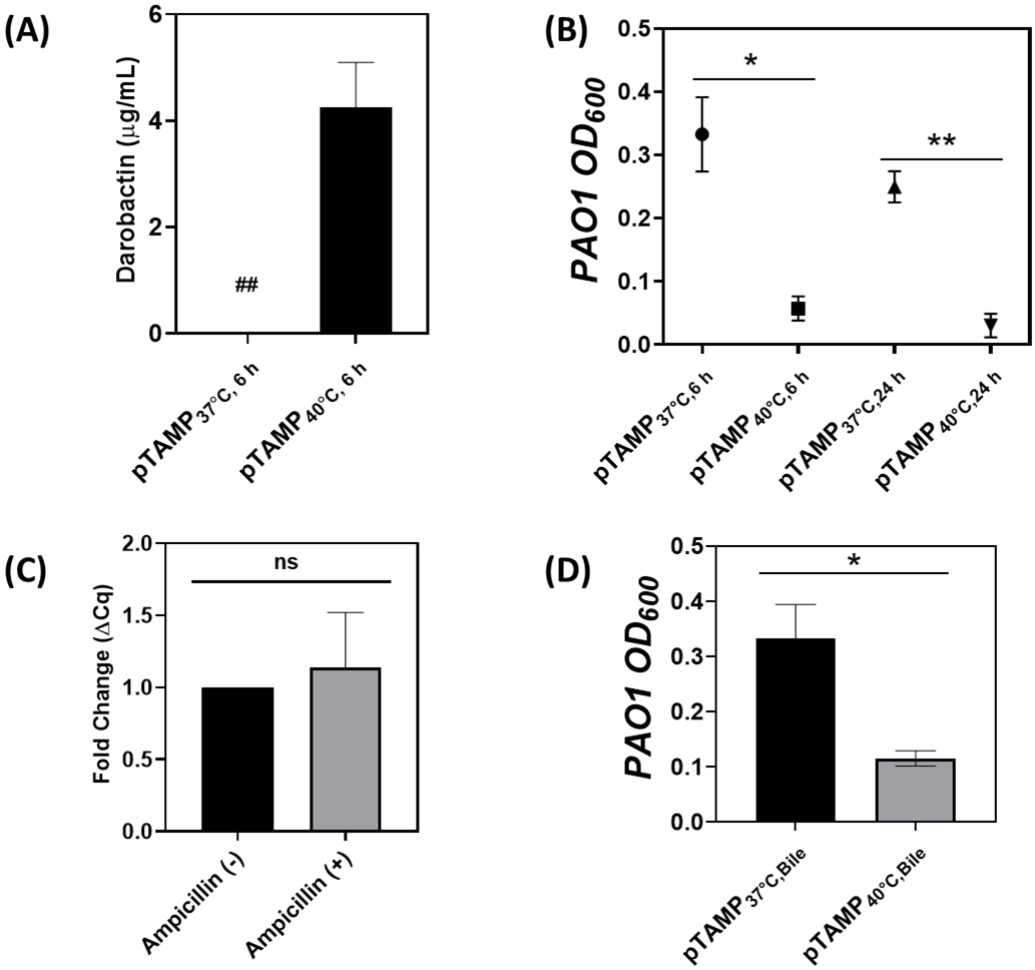

Figure 4. (A) Darobactin concentration in the liquid medium (in µg/mL) for the pTAMP-DarA-AT construct after 6 h of incubation at 37°C and 40°C. The error bars represent standard deviation based on three independent measurements. (##) represents darobactin concentrations lower than the Limit of Detection (LOD) by ESI-MS. (B) End-point absorbance (OD_{600}) of *P. aeruginosa* PAO1 after 18 h incubation at 37°C in filter-sterilized FM sustaining the growth of pTAMP-DarA-AT EcN strain. The FM collected from the 40°C incubated samples show a higher rate of *P. aeruginosa* PAO1 growth inhibition. The error bars represent standard deviation based on three independent measurements (*p = 0.0253; **p = 0.0093 as calculated by paired t-test) (C) qPCR analysis-based determination for the presence of pTAMP-DarA-AT recombinant plasmid in EcN with and without ampicillin (100

μg/mL) supplementation at 40°C, compared over 10 and 50 generation numbers. The error bars represent standard deviation based on three independent measurements. (D) End-point absorbance (OD_{600}) of *P. aeruginosa* PAO1 after 18 h incubation at 37°C in filter-sterilized FM containing 0.3% (w/v) bovine bile sustaining the growth of pTAMP-DarA-AT EcN strain. The error bars represent standard deviation based on three independent measurements (*p = 0.0185 as calculated by paired t-test).

Discussion

In this study, we have demonstrated the challenges in regulating the production of an enzymatically synthesized novel antibiotic and developed a solution to overcome those challenges. Specifically, we show how one inducible system (IPTG) results in high level production of darobactin but also suffers from significant basal level expression. This basal level expression can occur due to the affinity of the lacI repressor protein to related auto-inducer molecules, like lactose (disaccharide) and galactose (monosaccharide) present in the growth media as reported previously (Xu et al., 2012). Such cross-reactivity to simple carbohydrates cannot be reasonably avoided when pathogen inhibition is to be tested under therapeutically-relevant conditions. On the other hand, such cross-reactivity does not occur in the TlpA-based thermoresponsive genetic switch (Piraner et al., 2017b) but its transcriptional limitations can restrict heterologous protein production in the microbial chassis and reduce their application potential. This was observed in our case, where the standard thermal induction circuit could not reach the expected darobactin production levels in the liquid medium that was observed for the IPTG inducible system. By combining components from both systems, we developed a thermo-amplifier circuit that achieved undetectable levels of leaky production and high levels of thermally induced darobactin production in the growth medium. This was done by exploiting the strong transcriptional rate of the T7 promoter as previously reported for the opto-T7RNAP and related systems (Raghavan et al. 2020; Fernandez-Rodriguez et al., 2017). For the first time, we combined thermo-genetics with the prolific strength of the T7RNAP-T7 promoter combination and demonstrated the superior performance of this circuit for darobactin production. This thermo-amplifier circuit was encoded in a plasmid containing toxin-antitoxin system that is independent of antibiotic additives and can be kept stable in probiotic EcN.

It is to be noted that all these components were encoded in a single plasmid for ease of manipulation and testing across different *E. coli* strains. Apart from that, the presence of genes encoding for darobactin exporter enzymes in the recombinant plasmid also increased the darobactin tolerance of the EcN as shown by the MIC values (>16 µg/mL compared to 1.6 µg/mL of wild type EcN) without affecting the growth, which is consistent with the results previously observed for a standard *E. coli* BL21 (DE3) strain (Groß et al., 2021). Previous reports have shown considerable improvements in engineering *E.* coli-based strains, to sense and eliminate *P. aeruginosa* PAO1, both under *in-vitro* (Saeidi et al., 2011) and *in-vivo* (Hwang et al., 2018) conditions. The engineered strains could detect low levels of the quorum sensing molecule, N-acyl homoserine lactone ($3OC_{12}$-HSL) and undergo auto-lysis to release anti-*P. aeruginosa* toxin, pyocin S5 and reduce gut infections in animal models. As pointed out by Hwang and co-workers engineered EcN strains could colonize the mice intestine for a period of 3 weeks, which provided an extended temporal window to facilitate complete pathogen clearance. This attribute of the EcN strain combined with our thermoamplifier circuit might have potential to allow thermally regulated, sustained production of darobactin in *in-vivo* conditions. Another potential concern for the application of engineered EcN in the gut environment is the presence of the 52-kb polyketide synthase (*pks*) pathogenicity island in the bacterial genome that encodes for the genotoxin, colibactin (Homburg et al., 2007; Bian et al., 2013). Although there is evidence to show that colibactin can cause mutational damage in mice models (Nougayrède et al., 2021), the notion that it can cause long-term adverse effects is generally contested by parallel studies (Kalantari et al., 2023). However, the scientific community employing EcN to deliver therapeutics (nanobodies, cytokines, antibiotics) in the gut environment is gradually transitioning towards using the non-genotoxic, colibactin-free Δ*clb* EcN strain for developing LBPs that show pre-clinical efficacy (Lynch et al., 2023). Testing the performance of our genetic circuit in such a strain, would not only demonstrate its therapeutic potential but also expedite its usage for *in-vivo* applications, keeping in mind the long-term interest of both patients and the regulatory authorities.

Finally, this thermo-amplifier circuit could potentially be adapted to achieve highly regulated production of other enzymatically synthesized therapeutic compounds, for

example those biosynthesized by RiPP BGC. In recent years, the discovery of bioactive RiPPs and the elucidation of their biosynthesis has accelerated explosively and their encoding BGCs offer the advantage of relatively small size (Zhong et al., 2022). For example, the biosynthesis of bottromycin has now been clarified (Huo et al., 2012; Franz et al., 2021), a RiPP whose antibacterial activity against *Staphylococcus spp.* raises hopes for the further development of bottromycins as "living therapeutics".

Materials and Methods

Media, Bacterial Strains and Growth Conditions

Luria-Bertani (LB) and Mueller-Hinton (MHI) bacterial growth media used for this study were procured from Carl-Roth. Unfractionated Bovine Bile (CAS No – 8008-63-7, B3883-25G) was purchased from Merck Millipore GmbH, Germany. NEB® 5-alpha Competent *E. coli* cells (C2987H) were routinely used for recombinant plasmid cloning and maintenance. The thermoamplifier constructs were assembled in chemically competent ABLE-K cells (200172) procured from Agilent Technologies (USA). Clearcoli BL21 DE3 cells were obtained from BioCat GmbH (Heidelberg, Germany) and the alanine auxotrophic *ΔalrΔdadx* Clearcoli BL21 DE3 strain was created by Gen-H GmbH (Heidelberg, Germany). Clearcoli were grown in Luria-Bertani (LB) broth supplemented with 2% (w/v) sodium chloride, with additional supplementation of 40 µg/mL D-alanine for *ΔalrΔdadx* Clearcoli. *E. coli* Nissle 1917 (EcN) was isolated from commercially available Mutaflor® (Germany). *P. aeruginosa* PAO1 (22644) was obtained from DSMZ GmbH (Braunschweig, Germany).

Molecular Biology Reagents and Oligonucleotides

Q5 DNA Polymerase was used for DNA amplification and colony PCR screening (New England Biolabs, Germany). Gibson Assembly and site-directed mutagenesis was performed using the NEBuilder HiFi DNA Assembly Cloning Kit (E5520S) and KLD

Enzyme Mix (M0554S) respectively. Qiagen Plasmid Kit (12125) was used for plasmid extraction and Wizard® SV Gel and PCR Clean-Up System (A9282) was used for DNA purification. Oligonucleotides used in this study were synthesized from Integrated DNA Technologies (IDT, Belgium) and recombinant plasmids were verified by Sanger Sequencing (Eurofins, Germany).

Competent Cell Preparation

Electrocompetent cells of Clearcoli and *Δalr Δdadx* Clearcoli (alanine auxotroph) were prepared by repeated washing of bacterial pellet harvested at early exponential growth phase with 10% glycerol (v/v). Plasmids (500 ng) were transformed in the competent cells by electroporation at 1.8 kV, using 0.1 cm electroporation cuvettes (1652083) in the Bio-Rad MicropulserTM Electroporator. To prepare chemically competent EcN and EcN-T7 cells, bacterial cultures were grown overnight in LB broth at 37°C, 250 rpm and subcultured in 100 mL of fresh LB media [1:100 (v/v) dilution]. The cultures were incubated at 37 °C, 250 rpm until an OD_{600} = 0.4 was reached. The bacteria were pelleted down by centrifugation at 4000 rpm (3363 X g), 4 °C for 15 min and the supernatant was discarded. The bacterial pellet was then washed twice with ice-cold $CaCl_2$ (200 mM) and once with a 1:1 mixture of $CaCl_2$ (200 mM) and glycerol (10% w/v). After the final wash, the pellet was resuspended in 1 mL of $CaCl_2$+glycerol mixture and stored at -80°C as 100 µL aliquots. For bacterial transformation, 1 µg of the plasmids were added to the competent cells and gently mixed by flicking. The competent cells were then chilled on ice for 30 min and transferred to a 42 °C water bath for 45 s, followed by incubation on ice for 2 min. SOC media (900 µL) was added and mixed, and the cell suspension was incubated at 37 °C, 250 rpm for an hour before plating on LB agar with appropriate antibiotics.

Cultivation of the darobactin production strains

Recombinant strains were inoculated into LB (for EcN and EcN-T7 variants) and LB-NaCl (for Clearcoli BL21 DE3 variants) from the glycerol stocks and cultivated overnight at

30°C, 250 rpm with appropriate antibiotics. The bacterial suspensions were then subcultured in 25 mL of fresh Formulated Media (FM) [Composition - (K_2HPO_4 - 12.54 g/L, KH_2PO_4 – 2.31 g/L, D-Glucose – 4 g/L, NH_4Cl – 1 g/L, Yeast Extract – 12 g/L, NaCl – 5 g/L, $MgSO_4$ – 0.24 g/L) in a sterile glass conical flask (250 mL) at a 1:25 (v/v) ratio. The samples were kept at temperatures 37°C and 40°C for different temporal periods. For IPTG inducible conditions, 0.5 mM (500 µM) IPTG was added to the cultures at OD_{600}=0.4. Growth Curve of the strains were obtained by measuring OD_{600} at different time intervals using the Microplate Reader Infinite 200 Pro (Tecan Deutschland GmbH, Germany). For analyzing the bile tolerance of the production strain, the bacterial cultures were cultivated in FM supplemented with filter sterilized 0.3% (w/v) Bovine Bile at their respective incubation temperatures for 24 h.

Production and purification of darobactin A

The production and purification of darobactin A was performed as described previously for darobactin D (Seyfert et al., 2023b).

Electrospray Ionization - Mass Spectrometry (ESI-MS) based darobactin quantification

For figures 1B, 1D, 2B and 2D, the following method was used: LC/ESI QTOF-MS analysis is performed on a 1260 Infinity LC in combination with a 6545A high-resolution time-of-flight mass analyzer, both from Agilent Technologies (Santa Barbara, CA, USA). Separation of 1 µl of sample is performed using a Poroshell HPH-C18 column (3.0 x 50 mm, 2.7 µm) equipped with the same guard column (3.0 x 5 mm, 2.7 µm) by a linear gradient from (A) ACN + 0.1% formic acid to (B) water + 0.1% formic acid at a flow rate of 500µl/min and a column temperature of 45°C. Gradient conditions are as follows: 0-0.5min, 95% B; 0.5-6min, 95-60.5% B; 6-9.5 min 60.5-20% B at 1500 µl/min (column cleaning), 9.5-13min 95% B down to 500µl/min (equilibrium).

After separation, the LC flow enters the dual AJS ESI source set to 3500 V as capillary voltage, 40 psi nebulizer gas pressure and 7 l/min dry gas flow, and 300 °C dry gas

temperature. The TOF parameters used are high resolution mode (4 GHz), 140 V fragmentor and 45 V skimmer voltage. The mass spectra are acquired in the time interval of 2-6 min in full scan mode in the range m/z 150-3000 with a spectra rate of 4/s. For quantification of the Darobactin, the positive charged mass [M+2H]2+ at m/z 483.7089 Da were extracted and automatically integrated using Mass Hunter software.

Standards were prepared from Darobactin stock solution of 100 µg/ml in mobile phase (5%A, 95%B) or blank media. Calibration was done between 0 and 1 µg/ml or 0 and 10 µg/ml with recovery rates 97-105%. For analyzing real samples, the bacterial biomass was removed post-incubation by centrifugation [4000 rpm (3363Xg), 30 min, 4 °C] and the respective supernatants were filter-sterilized with 0.22 µm filters (Carl Roth, Germany) and provided with respective controls.

For the data in Figures 3B and 4A, the following method was used: Darobactin was quantified using a Vanquish Flex UHPLC (Thermo Fisher, Dreieich, Germany), coupled to a TSQ Altis Plus mass spectrometer (Thermo Fisher, Dreieich, Germany). Samples were diluted 1:10 in PBS pH 7.4, followed by addition of 2 volumes 10%MeOH/ACN containing 15 nM diphenhydramine as internal standard. Samples were centrifuged (15 min, 4°C, 4000 rpm) before analysis and darobactin content quantified in SRM mode using a calibration curve up to 5 µM. LC conditions were as follows: column: Hypersil GOLD C-18 (1.9 µm, 100 x 2.1 mm; Thermo Fisher, Dreieich, Germany); temperature 40°C; flow rate 0.700 ml/min; solvent A: water + 0.1% formic acid; solvent B: acetonitrile + 0.1% formic acid; gradient: 0-0.2 min 10% B, 0.2-1.2 min 10-90% B, 1.2-1.6 min 90% B, 1.6-2.0 min 10% B. MS conditions were as follows: vaporizer temperature 350°C, ion transfer tube temperature 380°C, Sheath Gas 30, Aux Gas 10, Sweep Gas 2; spray voltage: 4345 V, mass transition: 483.75 – 475.083 ($[M+2H]^{2+}$), collision energy: 11.0 V; Tube lens offset 55 V.

P. aeruginosa PAO1 Survival Assay

P. aeruginosa PAO1 was inoculated into 5 mL FM from glycerol stock and subjected to overnight incubation at 37°C with 180 rpm orbital shaking. The following day, *P. aeruginosa* PAO1 was subcultured in fresh FM at 1:50 ratio (v/v) and grown till it reached log phase (OD_{600}=0.4). The log-phase bacteria were further diluted in FM to optimize the bacterial cell number to $55X10^5$ CFU/mL. 10 µl of diluted bacterial culture were added to 100 µL of filter-sterilized supernatants (mentioned above) in a sterile 96-well U-bottom transparent plate (REF 351177, Corning, USA) to bring the final bacterial cell number to $5X10^5$ CFU/mL. The plates were incubated under static conditions for 18 h at 37°C and bacterial growth was determined by measuring absorbance at 600 nm in Microplate Reader Infinite 200 Pro (Tecan Deutschland GmbH, Germany).

qRT-PCR Analysis for Gene Expression

Bacterial cultures were cultivated in 5 mL of LB media (supplemented with 100 µg/mL ampicillin) at 30°C with continuous shaking (120 rpm). The following day, the bacterial suspension was subcultured in 25 mL of FM without any antibiotic supplementation in a 1:25 (v/v) ratio. Post 6 h incubation at the respective temperatures, the OD_{600} was determined using the NanoDrop Microvolume UV–Vis Spectrophotometer (ThermoFisher Scientific GmbH, Germany). All the bacterial cultures were normalized to OD_{600} of 0.8 to maintain an equivalent cell count. The normalized cultures were centrifuged at 13,000 rpm (16200Xg) and washed thrice with sterile Dulbecco's 1× PBS (Phosphate Buffer Saline) solution. The bacterial pellet was then resuspended in 1X DNA/RNA protection reagent supplied with the Monarch Total RNA Miniprep Kit (NEB #T2010) (New England BioLabs, USA) and subjected to mechanical lysis using the FastPrep-24™ 5G bead beating grinder system (MP Biomedicals Germany GmbH). Total RNA was isolated according to the manufacturer guidelines and measured at 260 nm to determine the net yield and purity. 500 ng of the total RNA from all extracted samples were then immediately converted into cDNA using the Thermo-Scientific Revertaid first strand cDNA synthesis kit (#K1622). Real time qPCR was performed using the iTaq™ Universal SYBR ® Green

Supermix (BioRad GmbH, Germany) in the Bio-Rad CFX96 Real time system C1000 Touch thermal cycler to determine the gene expression level of target genes. Bacterial 16S rRNA levels were also measured for all the samples as a control (Smati et al., 2013). The specific sequences of qRT-PCR primers are listed in Table S1. The quantification curve (Cq) values were selected by the regression determination mode and the mean ΔCq values were determined by the following formula: - ΔCq= Cq (37°C) – Cq (40°C). The data were finally represented in the form of fold change calculated as $2^{\Delta Cq}$.

qPCR Analysis for Plasmid Retention

Bacterial cultures were cultivated in 5 mL of LB media (supplemented with 100 µg/mL ampicillin) at 30°C with continuous shaking (120 rpm). The following day, the bacterial suspension was subcultured in 25 mL of FM both with and without antibiotic supplementation (100 µg/mL ampicillin) in a 1:25 (v/v) ratio. Bacterial cultures were immediately kept at 40°C and incubated for 24 h. Post 24 h incubation, the OD_{600} was measured, and fresh FM cultures were inoculated with the respective bacterial cultures at a starting OD_{600} of 0.01. This procedure was repeated over 5 days, resulting in 50 consecutive bacterial generations.

For qPCR analysis, 1 mL of the bacterial samples after every 10 generations were normalized to OD_{600} of 0.8 with sterile PBS. The normalized cultures were centrifuged at 13,000 rpm (16200Xg) and washed thrice with sterile Dulbecco's 1× PBS (Phosphate Buffer Saline) solution. 500 µl of the bacterial samples were then kept at 98°C for 15 min to undergo lysis in a static thermomixer (Eppendorf GmbH, Germany) according to the reported protocol (Škulj et al., 2008). The samples were then stored at -20°C for further analysis. Post collection of these bacterial samples till 50 generations, qPCR was performed using the iTaq™ Universal SYBR ® Green Supermix (BioRad GmbH, Germany) in the Bio-Rad CFX96 Real time system C1000 Touch thermal cycler. To prevent sample heterogeneity, qPCR reactions were conducted with primers specific to the pUC replication origin of the recombinant plasmid (listed in Supplementary Table S1). The specific sequences of qPCR primers are listed in Table S1. The quantification curve (Cq) values were selected by the regression determination mode and the mean ΔCq was

determined by the following formula: - ΔCq= Cq (50th generation) – Cq (10th generation). The data were finally represented in the form of fold change calculated as - Mean ΔCq (With Ampicillin)/Mean ΔCq (Without Ampicillin).

Acknowledgement

This work was supported by the Leibniz Science Campus on Living Therapeutic Materials [LifeMat]. We would like to thank Mikhail Shapiro for the pTlpA39-mWasabi plasmid (Addgene #86116), Chris Barnes for the pUC-GFP AT plasmid (Addgene #133306) and Paul Freemont for the mBP-T7RNAP plasmid (Addgene #74096). We thank Nicole Frankenberg-Dinke for providing us with the EcN-T7 strain (DSMZ 115365). We thank Andreas Kany for his help with the ESI-MS analysis of darobactin samples, and Sanjana Balaji Kuttae for her help in recombinant plasmid construction. All the schematic figures were generated using Biorender.

Conflict of Interest:

Rolf Müller and Carsten E. Seyfert are inventors of patent application WO2022175443A1, titled “Novel darobactin derivatives”.

References

1. Maxmen, A., 2017. Living therapeutics: Scientists genetically modify bacteria to deliver drugs (vol 23, pg 5, 2017). *NATURE MEDICINE*, *23*(3), pp.269-269.
2. Charbonneau, M.R., Isabella, V.M., Li, N. and Kurtz, C.B., 2020. Developing a new class of engineered live bacterial therapeutics to treat human diseases. *Nature Communications*, *11*(1), p.1738.
3. Liu, Y., Feng, J., Pan, H., Zhang, X. and Zhang, Y., 2022. Genetically engineered bacterium: Principles, practices, and prospects. *Frontiers in Microbiology*, *13*, p.997587.

4. Kelly, V.W., Liang, B.K. and Sirk, S.J., 2020. Living therapeutics: the next frontier of precision medicine. *ACS synthetic biology*, *9*(12), pp.3184-3201.
5. Omer, R., Mohsin, M.Z., Mohsin, A., Mushtaq, B.S., Huang, X., Guo, M., Zhuang, Y. and Huang, J., 2022. Engineered bacteria-based living materials for biotherapeutic applications. *Frontiers in Bioengineering and Biotechnology*, *10*, p.870675.
6. Rodrigo-Navarro, A., Sankaran, S., Dalby, M.J., del Campo, A. and Salmeron-Sanchez, M., 2021. Engineered living biomaterials. *Nature Reviews Materials*, *6*(12), pp.1175-1190.
7. Zhou, Y. and Han, Y., 2022. Engineered bacteria as drug delivery vehicles: principles and prospects. *Engineering Microbiology*, *2*(3), p.100034.
8. Kan, A., Gelfat, I., Emani, S., Praveschotinunt, P. and Joshi, N.S., 2020. Plasmid vectors for in vivo selection-free use with the probiotic E. coli Nissle 1917. *ACS synthetic biology*, *10*(1), pp.94-106.
9. Abedi, M.H., Yao, M.S., Mittelstein, D.R., Bar-Zion, A., Swift, M.B., Lee-Gosselin, A., Barturen-Larrea, P., Buss, M.T. and Shapiro, M.G., 2022. Ultrasound-controllable engineered bacteria for cancer immunotherapy. *Nature Communications*, *13*(1), p.1585.
10. Li, L., Pan, H., Pang, G., Lang, H., Shen, Y., Sun, T., Zhang, Y., Liu, J., Chang, J., Kang, J. and Zheng, H., 2022. Precise thermal regulation of engineered bacteria secretion for breast cancer treatment in vivo. *ACS Synthetic Biology*, *11*(3), pp.1167-1177.
11. Sankaran, S., Becker, J., Wittmann, C. and Del Campo, A., 2019. Optoregulated drug release from an engineered living material: self-replenishing drug depots for long-term, light-regulated delivery. *Small*, *15*(5), p.1804717.
12. Sugianto, W., Altin-Yavuzarslan, G., Tickman, B.I., Kiattisewee, C., Yuan, S.F., Brooks, S.M., Wong, J., Alper, H.S., Nelson, A. and Carothers, J.M., 2023. Gene expression dynamics in input-responsive engineered living materials programmed for bioproduction. *Materials Today Bio*, *20*, p.100677.
13. Imai, Y., Meyer, K.J., Iinishi, A., Favre-Godal, Q., Green, R., Manuse, S., Caboni, M., Mori, M., Niles, S., Ghiglieri, M. and Honrao, C., 2019. A new antibiotic selectively kills Gram-negative pathogens. *Nature*, *576*(7787), pp.459-464.

14. Seyfert, C.E., Porten, C., Yuan, B., Deckarm, S., Panter, F., Bader, C.D., Coetzee, J., Deschner, F., Tehrani, K.H., Higgins, P.G. and Seifert, H., 2023. Darobactins exhibiting superior antibiotic activity by Cryo-EM structure guided biosynthetic engineering. *Angewandte Chemie International Edition*, *62*(2), p.e202214094.
15. Li, X., Ma, S. and Zhang, Q., 2023. Chemical Synthesis and Biosynthesis of Darobactin. *Tetrahedron Letters*, p.154337.
16. Wuisan, Z.G., Kresna, I.D.M., Böhringer, N., Lewis, K. and Schäberle, T.F., 2021. Optimization of heterologous Darobactin A expression and identification of the minimal biosynthetic gene cluster. *Metabolic Engineering*, *66*, pp.123-136.
17. Groß, S., Panter, F., Pogorevc, D., Seyfert, C.E., Deckarm, S., Bader, C.D., Herrmann, J. and Müller, R., 2021. Improved broad-spectrum antibiotics against Gram-negative pathogens via darobactin biosynthetic pathway engineering. *Chemical science*, *12*(35), pp.11882-11893.
18. Seyfert, C.E., Müller, A.V., Walsh, D.J., Birkelbach, J., Kany, A.M., Porten, C., Yuan, B., Krug, D., Herrmann, J., Marlovits, T.C. and Hirsch, A.K., 2023. New Genetically Engineered Derivatives of Antibacterial Darobactins Underpin Their Potential for Antibiotic Development. *Journal of Medicinal Chemistry*.
19. Piraner, D.I., Abedi, M.H., Moser, B.A., Lee-Gosselin, A. and Shapiro, M.G., 2017. Tunable thermal bioswitches for in vivo control of microbial therapeutics. *Nature chemical biology*, *13*(1), pp.75-80.
20. Mamat, U., Wilke, K., Bramhill, D., Schromm, A.B., Lindner, B., Kohl, T.A., Corchero, J.L., Villaverde, A., Schaffer, L., Head, S.R. and Souvignier, C., 2015. Detoxifying Escherichia coli for endotoxin-free production of recombinant proteins. *Microbial cell factories*, *14*, pp.1-15.
21. Nguyen, H., Made Kresna, I.D., Böhringer, N., Ruel, J., Mora, E.D.L., Kramer, J.C., Lewis, K., Nicolet, Y., Schäberle, T.F. and Yokoyama, K., 2022. Characterization of a radical SAM oxygenase for the ether crosslinking in darobactin biosynthesis. *Journal of the American Chemical Society*, *144*(41), pp.18876-18886.
22. Basaran, S., Dey, S., Bhusari, S., Sankaran, S. and Kraus, T., 2023. Plasmonic stimulation of gold nanorods for the photothermal control of engineered living materials. *Biomaterials Advances*, *147*, p.213332.

23. Singha, T.K., Gulati, P., Mohanty, A., Khasa, Y.P., Kapoor, R.K. and Kumar, S., 2017. Efficient genetic approaches for improvement of plasmid based expression of recombinant protein in Escherichia coli: A review. *Process Biochemistry*, *55*, pp.17-31.
24. Landry, B.P. and Tabor, J.J., 2018. Engineering diagnostic and therapeutic gut bacteria. *Bugs as Drugs: Therapeutic Microbes for the Prevention and Treatment of Disease*, pp.331-361.
25. Aggarwal, N., Breedon, A.M.E., Davis, C.M., Hwang, I.Y. and Chang, M.W., 2020. Engineering probiotics for therapeutic applications: recent examples and translational outlook. *Current opinion in biotechnology*, *65*, pp.171-179.
26. Durmusoglu, D., Al'Abri, I., Li, Z., Islam Williams, T., Collins, L.B., Martínez, J.L. and Crook, N., 2023. Improving therapeutic protein secretion in the probiotic yeast Saccharomyces boulardii using a multifactorial engineering approach. *Microbial Cell Factories*, *22*(1), pp.1-18.
27. Hwang, I.Y., Koh, E., Wong, A., March, J.C., Bentley, W.E., Lee, Y.S. and Chang, M.W., 2017. Engineered probiotic Escherichia coli can eliminate and prevent Pseudomonas aeruginosa gut infection in animal models. *Nature communications*, *8*(1), p.15028.
28. Gurbatri, C.R., Lia, I., Vincent, R., Coker, C., Castro, S., Treuting, P.M., Hinchliffe, T.E., Arpaia, N. and Danino, T., 2020. Engineered probiotics for local tumor delivery of checkpoint blockade nanobodies. *Science translational medicine*, *12*(530), p.eaax0876.
29. Grady, R. and Hayes, F., 2003. Axe–Txe, a broad-spectrum proteic toxin–antitoxin system specified by a multidrug-resistant, clinical isolate of Enterococcus faecium. *Molecular microbiology*, *47*(5), pp.1419-1432.
30. Fedorec, A.J., Ozdemir, T., Doshi, A., Ho, Y.K., Rosa, L., Rutter, J., Velazquez, O., Pinheiro, V.B., Danino, T. and Barnes, C.P., 2019. Two new plasmid post-segregational killing mechanisms for the implementation of synthetic gene networks in Escherichia coli. *Iscience*, *14*, pp.323-334.
31. Harimoto, T., Hahn, J., Chen, Y.Y., Im, J., Zhang, J., Hou, N., Li, F., Coker, C., Gray, K., Harr, N. and Chowdhury, S., 2022. A programmable encapsulation system

improves delivery of therapeutic bacteria in mice. *Nature Biotechnology*, *40*(8), pp.1259-1269.

32. Effendi, S.S.W. and Ng, I.S., 2022. Reprogramming T7RNA polymerase in Escherichia coli Nissle 1917 under specific lac operon for efficient p-coumaric acid production. *ACS Synthetic Biology*, *11*(10), pp.3471-3481.
33. Yu, M., Hu, S., Tang, B., Yang, H. and Sun, D., 2023. Engineering Escherichia coli Nissle 1917 as a microbial chassis for therapeutic and industrial applications. *Biotechnology Advances*, p.108202.
34. Fiege, K. and Frankenberg-Dinkel, N., 2020. Construction of a new T7 promoter compatible Escherichia coli Nissle 1917 strain for recombinant production of heme-dependent proteins. *Microbial Cell Factories*, *19*, pp.1-7.
35. Mortzfeld, B.M., Palmer, J.D., Bhattarai, S.K., Dupre, H.L., Mercado-Lubio, R., Silby, M.W., Bang, C., McCormick, B.A. and Bucci, V., 2022. Microcin MccI47 selectively inhibits enteric bacteria and reduces carbapenem-resistant Klebsiella pneumoniae colonization in vivo when administered via an engineered live biotherapeutic. *Gut Microbes*, *14*(1), p.2127633.
36. Reen, F.J., Flynn, S., Woods, D.F., Dunphy, N., Chróinín, M.N., Mullane, D., Stick, S., Adams, C. and O'Gara, F., 2016. Bile signalling promotes chronic respiratory infections and antibiotic tolerance. *Scientific reports*, *6*(1), p.29768.
37. Flynn, S., Reen, F.J. and O'Gara, F., 2019. Exposure to bile leads to the emergence of adaptive signaling variants in the opportunistic pathogen Pseudomonas aeruginosa. *Frontiers in microbiology*, *10*, p.2013.
38. Nakkarach, A., Foo, H.L., Song, A.A.L., Nitisinprasert, S. and Withayagiat, U., 2020. Promising discovery of beneficial Escherichia coli in the human gut. *3 Biotech*, *10*, pp.1-14.
39. Wheatley, R.M., Caballero, J.D., van der Schalk, T.E., De Winter, F.H., Shaw, L.P., Kapel, N., Recanatini, C., Timbermont, L., Kluytmans, J., Esser, M. and Lacoma, A., 2022. Gut to lung translocation and antibiotic mediated selection shape the dynamics of Pseudomonas aeruginosa in an ICU patient. *Nature communications*, *13*(1), p.6523.

40. Xu, J., Banerjee, A., Pan, S.H. and Li, Z.J., 2012. Galactose can be an inducer for production of therapeutic proteins by auto-induction using E. coli BL21 strains. *Protein expression and purification*, *83*(1), pp.30-36.
41. Piraner, D.I., Farhadi, A., Davis, H.C., Wu, D., Maresca, D., Szablowski, J.O. and Shapiro, M.G., 2017. Going deeper: biomolecular tools for acoustic and magnetic imaging and control of cellular function. *Biochemistry*, *56*(39), pp.5202-5209.
42. Raghavan, A.R., Salim, K. and Yadav, V.G., 2020. Optogenetic control of heterologous metabolism in E. coli. *ACS Synthetic Biology*, *9*(9), pp.2291-2300.
43. Fernandez-Rodriguez, J., Moser, F., Song, M. and Voigt, C.A., 2017. Engineering RGB color vision into Escherichia coli. *Nature chemical biology*, *13*(7), pp.706-708.
44. Saeidi, N., Wong, C.K., Lo, T.M., Nguyen, H.X., Ling, H., Leong, S.S.J., Poh, C.L. and Chang, M.W., 2011. Engineering microbes to sense and eradicate Pseudomonas aeruginosa, a human pathogen. *Molecular systems biology*, *7*(1), p.521.
45. Hwang, I.Y., Lee, H.L., Huang, J.G., Lim, Y.Y., Yew, W.S., Lee, Y.S. and Chang, M.W., 2018. Engineering microbes for targeted strikes against human pathogens. *Cellular and Molecular Life Sciences*, *75*, pp.2719-2733.
46. Homburg, S., Oswald, E., Hacker, J. and Dobrindt, U., 2007. Expression analysis of the colibactin gene cluster coding for a novel polyketide in Escherichia coli. *FEMS microbiology letters*, *275*(2), pp.255-262.
47. Bian, X., Fu, J., Plaza, A., Herrmann, J., Pistorius, D., Stewart, A.F., Zhang, Y. and Müller, R., 2013. In vivo evidence for a prodrug activation mechanism during colibactin maturation. *ChemBioChem*, *14*(10), pp.1194-1197.
48. Nougayrède, J.P., Chagneau, C.V., Motta, J.P., Bossuet-Greif, N., Belloy, M., Taieb, F., Gratadoux, J.J., Thomas, M., Langella, P. and Oswald, E., 2021. A toxic friend: genotoxic and mutagenic activity of the probiotic strain Escherichia coli Nissle 1917. *MSphere*, *6*(4), pp.e00624-21.
49. Kalantari, A., James, M.J., Renaud, L.A., Perreault, M., Monahan, C.E., McDonald, M.N., Hava, D.L. and Isabella, V.M., 2023. Robust performance of a live bacterial therapeutic chassis lacking the colibactin gene cluster. *PLoS One*, *18*(2), p.e0280499.
50. Lynch, J.P., González-Prieto, C., Reeves, A.Z., Bae, S., Powale, U., Godbole, N.P., Tremblay, J.M., Schmidt, F.I., Ploegh, H.L., Kansra, V. and Glickman, J.N., 2023.

Engineered Escherichia coli for the in situ secretion of therapeutic nanobodies in the gut. *Cell Host & Microbe*, *31*(4), pp.634-649.

51. Zhong, G., Wang, Z.J., Yan, F., Zhang, Y. and Huo, L., 2022. Recent Advances in Discovery, Bioengineering, and Bioactivity-Evaluation of Ribosomally Synthesized and Post-translationally Modified Peptides. *ACS bio & med Chem Au*, *3*(1), pp.1-31.
52. Huo, L., Rachid, S., Stadler, M., Wenzel, S.C. and Müller, R., 2012. Synthetic biotechnology to study and engineer ribosomal bottromycin biosynthesis. *Chemistry & biology*, *19*(10), pp.1278-1287.
53. Franz, L., Kazmaier, U., Truman, A.W. and Koehnke, J., 2021. Bottromycins-biosynthesis, synthesis and activity. Natural product reports, 38(9), pp.1659-1683.
54. Smati, M., Clermont, O., Le Gal, F., Schichmanoff, O., Jauréguy, F., Eddi, A., Denamur, E., Picard, B. and Coliville Group, 2013. Real-time PCR for quantitative analysis of human commensal Escherichia coli populations reveals a high frequency of subdominant phylogroups. *Applied and environmental microbiology*, *79*(16), pp.5005-5012.
55. Škulj, M., Okršlar, V., Jalen, Š., Jevševar, S., Slanc, P., Štrukelj, B. and Menart, V., 2008. Improved determination of plasmid copy number using quantitative real-time PCR for monitoring fermentation processes. *Microbial cell factories*, *7*(1), pp.1-12.
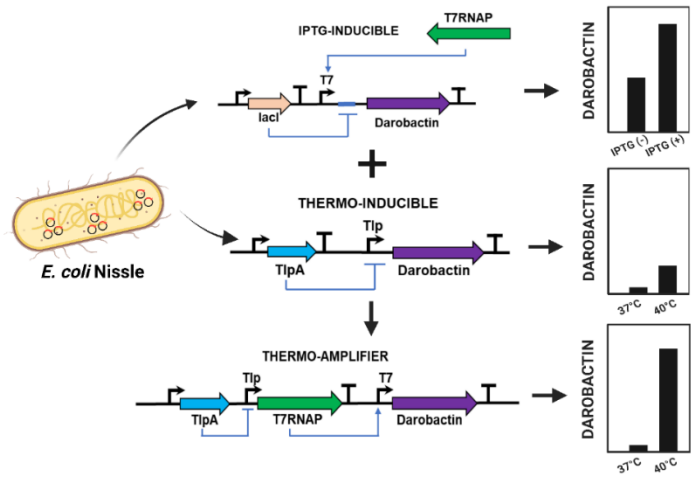
Graphical Abstract